

Among the fibers: A multimodality imaging review of intramuscular mass lesions

Karthik Shyam, Soumya Cicilet, Babu Philip

Department of Radiodiagnosis and Imaging, St. John's Medical College Hospital, Bengaluru, Karnataka, India

Correspondence: Dr. Karthik Shyam, #403, Third Floor, Mahaveer Palms Apartments, Kodichikkanahalli Main Road, Bengaluru - 560 076, Karnataka, India. E-mail: dr.karthikshyam@gmail.com

Abstract

The common presentations of patient complaints regarding the musculoskeletal system, such as pain, swelling, and restriction of movement, lead to the imaging discovery of various lesions often located in, or arising from, skeletal muscle in the region of interest. Knowledge of the patients' clinical history, laboratory parameters, and various imaging characteristics of the implicated lesions would assist the radiologist in coming to a timely, reasonably accurate conclusion about the etiology of the patient's complaints, the severity of disease, and in directing patient therapy.

Key words: Abscess; intramuscular; hemangioma; hematoma; lipoma; liposarcoma; myocystercosis; myositis ossificans; sarcoma; vascular malformation

Introduction

The common presentations of patient complaints regarding the musculoskeletal system lead to the imaging discovery of various lesions of skeletal muscle, of varied etiology, including traumatic, infectious, autoimmune, inflammatory, neoplastic, and iatrogenic. Imaging may help in their timely diagnosis, avoid unnecessary surgical intervention, and provide guidance for pathological diagnosis.

Intramuscular Abscesses

Infection and subsequent inflammation of muscle may be due to varied etiology, such as hematogenous septic seeding (bacterial, fungal), direct extension from a local source of infection (i.e., osteomyelitis, cellulitis), or via a

parallel autoimmune response to remote infection, such as in Lyme disease and influenza. The most common microbe implicated is *Staphylococcus aureus*, and in a Koch's endemic country like India, *Mycobacterium tuberculosis*.

On ultrasonography (USG), abscesses typically appear as variably defined heteroechoic collections, with internal debris and occasional septation. Enlargement of the affected muscle is seen. Perilesional vascularity is marked on color Doppler, and edema with inflammatory changes is noted to surround the lesion. On computed tomography (CT), enlargement of the muscle with surrounding fat-stranding is noted. The abscess *per se* appears as a focal hypodensity with peripheral rim enhancement with contrast, which helps differentiate it from myonecrosis, which does not show

This is an open access journal, and articles are distributed under the terms of the Creative Commons Attribution-NonCommercial-ShareAlike 4.0 License, which allows others to remix, tweak, and build upon the work non-commercially, as long as appropriate credit is given and the new creations are licensed under the identical terms.

For reprints contact: reprints@medknow.com

Cite this article as: Shyam K, Cicilet S, Philip B. Among the fibers: A multimodality imaging review of intramuscular mass lesions. Indian J Radiol Imaging 2018;28:214-24.

Access this article online

Quick Response Code:



Website:
www.ijri.org

DOI:
10.4103/ijri.IJRI_299_17

enhancement. On magnetic resonance (MR) [Figure 1], muscular enlargement with edema is present as T2 hyperintensity. The abscess appears T1-hypointense and T2-hyperintense, with peripheral contrast enhancement and occasional internal septation and fluid–fluid level [Figure 2A and B]. However, signal intensity may vary depending on the proportion of blood/proteinaceous material present within the cavity. This may cause confusion in the differentiation of abscesses and hematomata.

Though abscesses intuitively appear to present as acute collections, they may mimic a malignant mass lesion in the subacute or chronic clinical scenario. In such cases, cold abscesses caused by *M. tuberculosis* are to be considered. Occurring as a consequence to unmitigated infection of the vertebrae (i.e., Pott disease) [Figures 3 and 4], these muscular collections often coexist with destructive vertebral lesions and other stigmata of Koch's. On imaging, they are seen to appear similar to their acute counterparts.

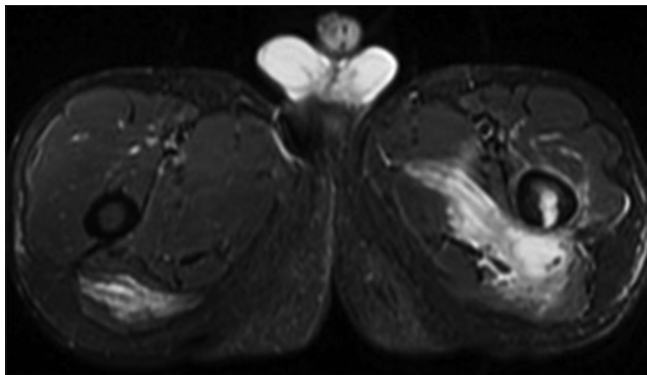


Figure 1: Femoral osteomyelitis in a 40-year-old male with left thigh pain. Axial STIR MR image of bilateral thighs shows left proximal medullary femoral hyperintensity with spread into the adductor and hamstring muscles. Incidental STIR hyperintensity of the right gluteus maximus noted after intramuscular injection administration

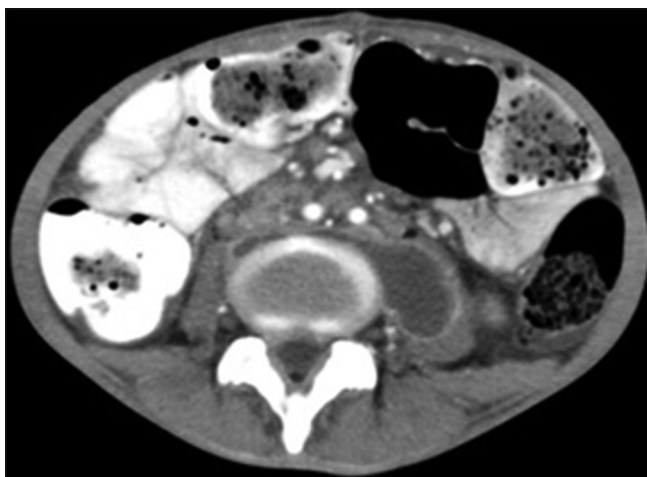


Figure 3: Cold abscess in a 42-year-old male with active pulmonary Koch's. Axial contrast-enhanced (CE) CT image shows a well-defined, peripherally enhancing hypodensity in the left psoas, crossing the midline. Aspirates revealed acid fast bacilli (AFB)

Intramuscular Benign Tumors

Lipoma

Lipomata are the most common benign mesenchymal soft-tissue tumors. Intramuscular lipomata are uncommon

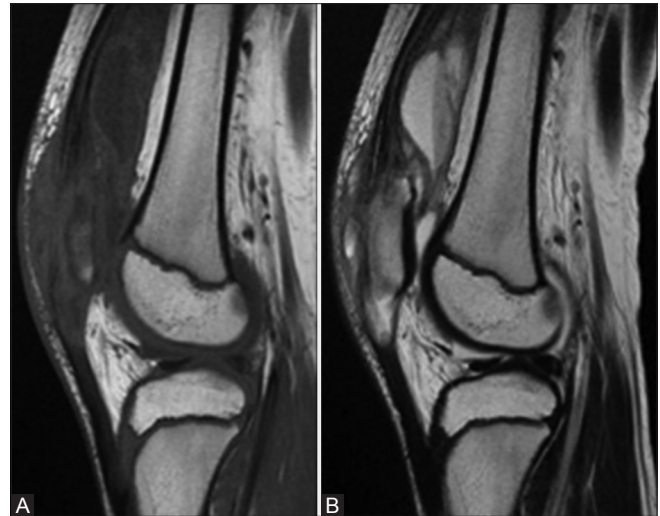


Figure 2 (A and B): Abscess within the quadriceps in a 20-year-old immunocompromised female. (A) Sagittal T1W and (B) sagittal T2W images of the thigh showing fluid–fluid level in a suppurative collection within the vastus intermedius

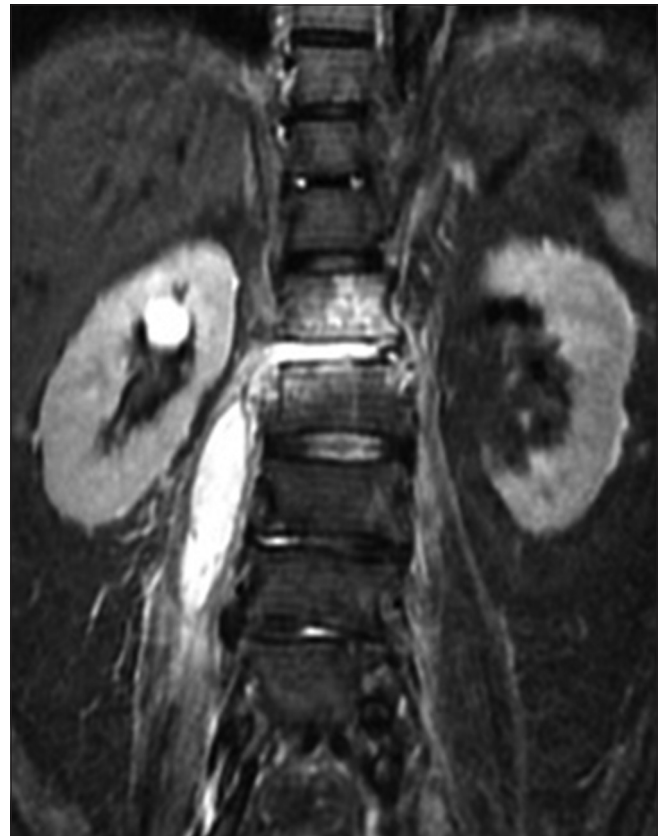


Figure 4: Cold abscess in a 67-year-old lady with lower back ache. Coronal MRI shows a T2/STIR hyperintense collection noted within the right psoas muscle, noted to extend from the L1-L2 intervertebral disc. Histopathology confirmed the presence of AFB. Incidentally noted is a right renal cyst

and constitute just over 1.8% of all primary tumors of adipose tissue and <1% of all lipomas.^[1] On ultrasound (US), they are usually well-defined, hyperechoic masses with scanty internal vascularity.^[2]

On CT [Figure 5], lipomata are usually well-defined and homogeneous, with a low tissue attenuation (approx. -65 to -120HU), without contrast enhancement. On MR imaging (MRI) [Figure 6A–D], the signal intensity of lesion parallels that of subcutaneous fat on all sequences, being hyperintense to skeletal muscle on both T1- (T1W) and T2-weighted (T2W) images.

Hemangioma

Hemangiomata frequently involve soft tissue. Soft-tissue hemangiomata are benign endothelial neoplasms that histologically resemble normal blood vessels. Intramuscular hemangiomata account for approximately 0.8% of all benign soft-tissue tumors.^[3] US can identify abnormal Doppler flow patterns or features consistent with phleboliths. Angiography may demonstrate the fine vascular details of a hemangioma, useful when embolization or surgical resection of complex lesions is considered. Presence of fat within a hemangioma is characteristic, and often serves to differentiate it from an intramuscular arteriovenous malformation (the latter of which tends to exhibit phleboliths). On MRI [Figure 7A–C], T1W images show an amorphous low-to-intermediate signal intensity mass with ill-defined margins due to peripheral flow voids and variable intralesional fat suppression [Figures 8A,B and 9A,B]. T2W images show low-signal intensity in areas of vascular components. Plain CT [Figure 7D] generally shows a poorly defined lesion with attenuation similar to that of skeletal muscle.

Neurofibroma

Neurofibromata [Figure 10A and B] are benign peripheral nerve sheath tumors, usually solitary and sporadic.

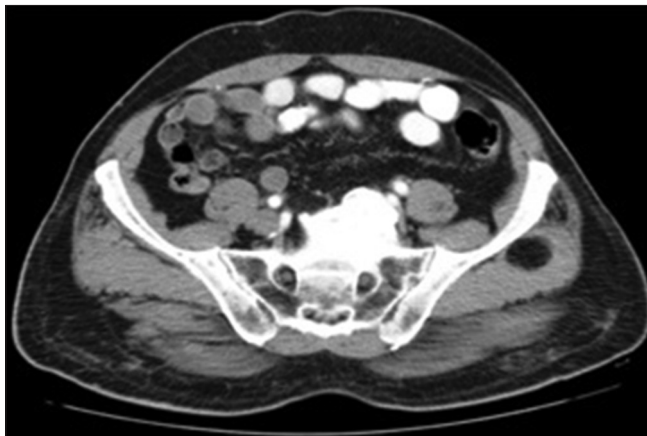


Figure 5: Lipoma incidentally discovered in a 22-year-old male. Axial CECT image shows a left gluteal intramuscular lipoma showing fat attenuation with no enhancement

A majority of cases are localized (90%), and not associated with neurofibromatosis Type 2.^[4] They may also be diffuse or plexiform, the latter being pathognomonic of neurofibromatosis Type 1. On CT, localized neurofibromata are well-defined, hypodense, and show little-to-no contrast enhancement. On MR, they appear T1-hypointense, T2-hyperintense, and show heterogeneous contrast enhancement.

Desmoid Fibromatosis

Desmoid fibromatoses [Figure 11A and B] are a rare (incidence of 0.03% of all neoplasms^[5]) broad group of fibroproliferative lesions that show myofibroblastic cells, dense collagen deposition, and variable myxoid stroma. Aggressive desmoid fibromas show local infiltrative growth and recurrence, but are unable to metastasize. They may occur in the fascial or musculo-aponeurotic planes. On USG, they have smooth, sharp margins with variable echogenicity; unenhanced CT may show a well-defined hyperattenuating intramuscular lesion with variable contrast enhancement. MR reveals hypointensity on T1 and T2 weighting, with moderate to marked contrast enhancement.

Myxoma

Intramuscular myxomas [Figure 12A–C] are a rare benign type of soft-tissue myxoma, which present as deep-seated masses composed of fibroblasts and abundant myxoid stroma. With an incidence of approximately 0.1 per 100,000, the average age of detection is 40–60 years predominantly in female patients.^[6] USG reveals a hypoechoic mass with a heterogeneous echotexture, often with posterior acoustic enhancement. On MR, it appears T1-hypointense,

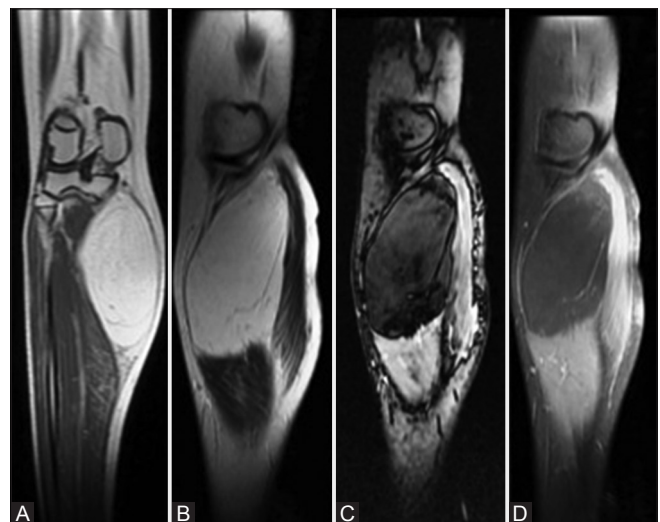


Figure 6 (A–D): Lipoma in a 30-year-old male with chronic, painless calf swelling. Coronal (A) T1W hyperintense, (B) T2W hyperintense, (C) sagittal STIR hypointense well-defined lesion within the medial head of gastrocnemius, exhibiting (D) fat suppression with minimal septal enhancement on sagittal CE T1W image

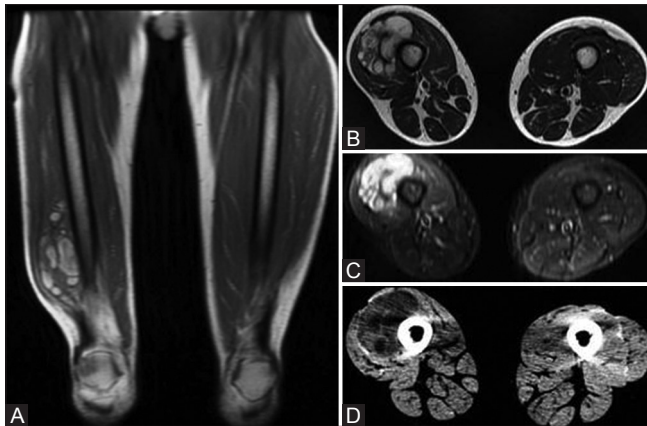


Figure 7 (A-D): Hemangioma in a 30-year-old male with painless swelling in the right thigh. (A) Coronal T1W shows a heterogeneously hyperintense lesion within right vastus lateralis; (B) Axial T2W and (C) axial STIR images show a heterogeneously hyperintense lesion; (D) Axial unenhanced CT image shows a hypoattenuating lesion

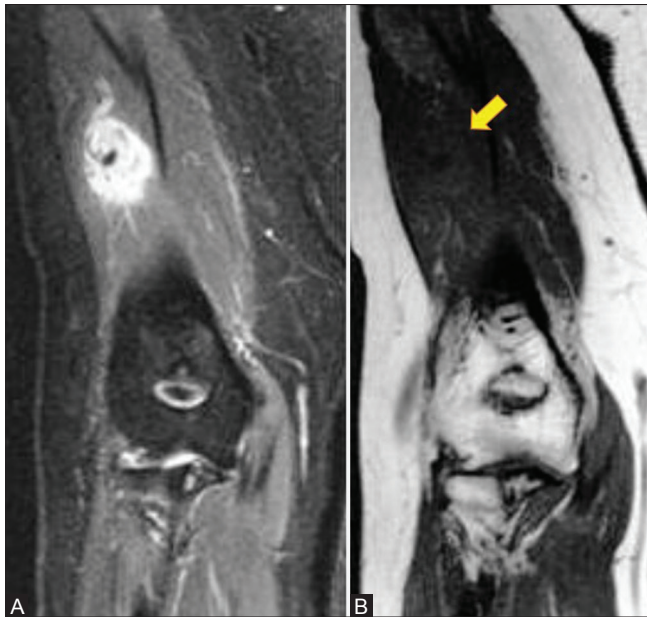


Figure 9 (A and B): Hemangioma in a 20-year-old male with painless swelling of the posterior compartment of arm. (A) Coronal STIR image shows a hyperintense lesion within the lateral head of the triceps; (B) Coronal T1W image shows a hypointense mass (arrow)

T2-hyperintense, and shows variable peripheral and internal contrast enhancement.^[7]

Hamartoma

Mesenchymal hamartomata [Figure 13A–D] are usually benign collection of heterotopically located mature soft tissue. They may contain muscular, lipomatous, fibrous, and neural components.

US reveals a homogeneously isoechoic, vascular lesion. On MRI, the lesion appears T1 iso-to-hypointense, and T2 and short inversion time inversion recovery (STIR) hyperintense.

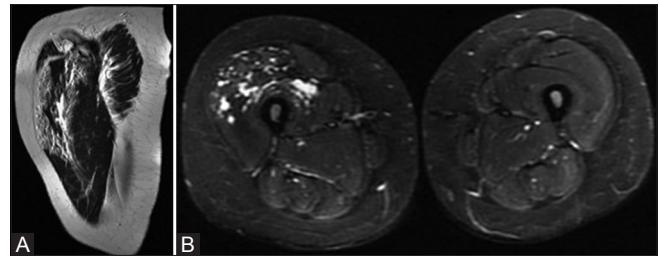


Figure 8 (A and B): Hemangioma in a 37-year-old female with right quadriceps weakness. (A) Axial STIR image shows a heterogeneously hyperintense intramuscular focus in the right quadriceps, with intralesional areas of fat suppression; (B) Sagittal T2W image shows an ill-defined intramuscular hyperintensity

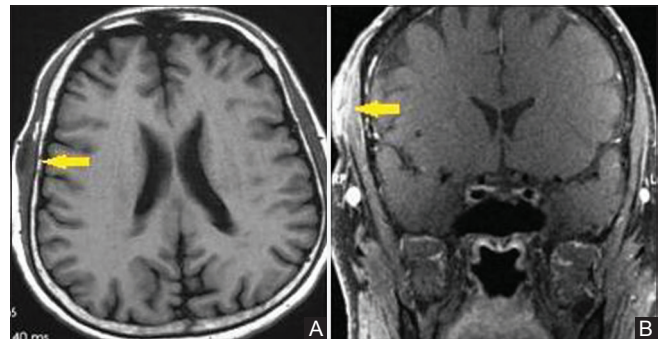


Figure 10 (A and B): Neurofibroma in a 60-year-old female with known orbital neurofibromatosis. (A) Axial T1W shows an isointense lesion (arrow) within the right temporalis muscle; (B) Coronal CE T1W image shows the lesion's heterogeneous enhancement

Heterogeneous enhancement is seen postcontrast. CT shows a well-defined hypodensity.

Typically, biopsy reveals fibromuscular and adipose tissue showing many proliferating, dilated, congested, thick, and thin-walled blood vessels, along with intramuscular adipose tissue, smooth muscle, and neural tissue, suggestive of a mesenchymal hamartoma.

Intramuscular Malignant Tumors

Soft-tissue sarcomas are a heterogeneous group of tumors that arise from tissue of mesenchymal origin and are characterized by infiltrative local growth.

Primary intramuscular malignant tumors

Rhabdomyosarcoma

Rhabdomyosarcomas are the most common soft-tissue tumor in children, and commonly occur in adults under the age of 45. On US [Figure 14D], muscular sarcomas (rhabdomyosarcomas) appear as an irregular, usually well-defined mass with low to intermediate echogenicity. Marked vascularity may be noted on color Doppler imaging.

On CT, these masses show soft-tissue attenuation with variable contrast enhancement. On MRI [Figure 14A–C],

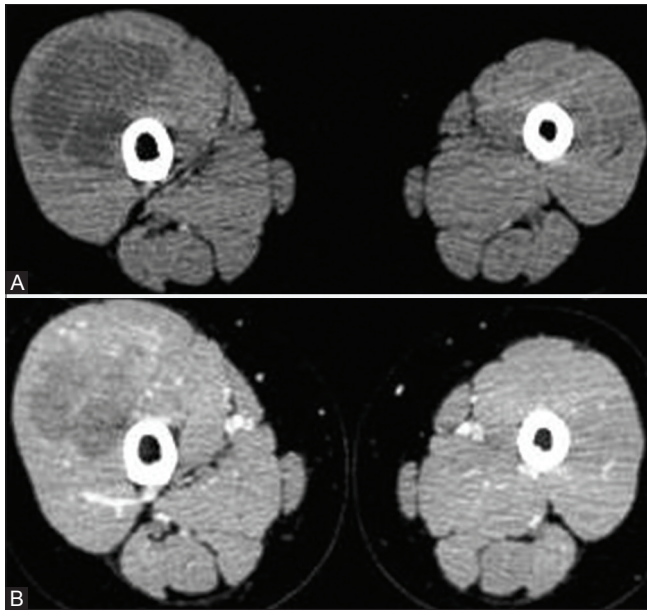


Figure 11 (A and B): Desmoid fibromatosis in a 56-year-old male with progressive weakness of the extensor compartment of right thigh. (A) Unenhanced axial CT image of the lower limbs shows a well-defined mass within the right vastus intermedius with extension to the vastus lateralis; (B) CE axial CT image shows the lesion's heterogeneous enhancement

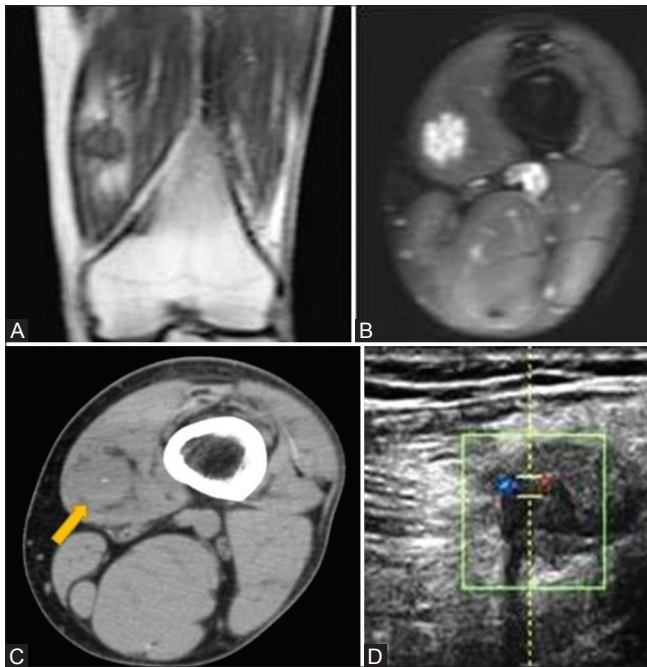


Figure 13 (A-D): Hamartoma in a 27-year-old female with pain in the medial compartment of left thigh. (A) Coronal T1W image shows a well-defined iso-hypointense lesion within the left vastus medialis; (B) Axial STIR image shows hyperintensity; (C) Axial CT reveals isointensity with speck of central calcification (arrow); (D) Ultrasound shows a vascular isoechoic lesion

they appear T1-hypointense and T2-hyperintense, with variable contrast enhancement. Foci of necrosis within the tumor herald a poor prognosis.

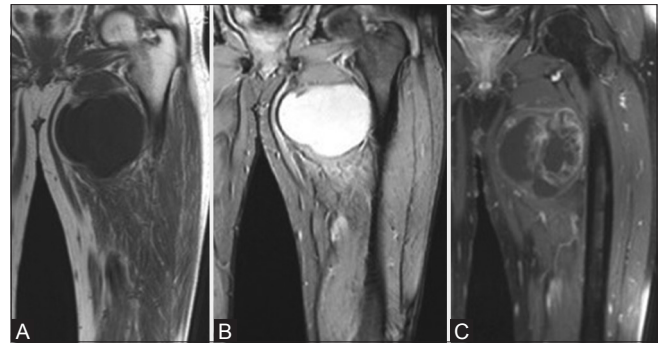


Figure 12 (A-C): Myxoma in a 48-year-old male with progressive left groin swelling. (A) Coronal T1W image shows a hypointense, well-defined lesion within the left adductor magnus; (B) Coronal T2W image shows a hyperintense mass; (C) CE coronal T1W image reveals the lesion's heterogeneous enhancement

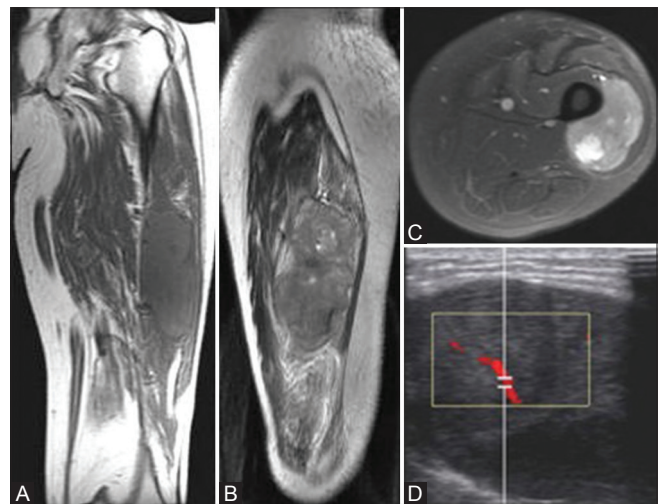


Figure 14 (A-D): Rhabdomyosarcoma in a 21-year-old male with rapidly progressive, painful swelling of the left thigh. (A) Coronal T1W image shows iso-intense lesion within left vastus lateralis; (B) Sagittal T2W image shows a hyperintense lesion, with necrosis; (C) Axial STIR image shows hyperintensity; (D) Hypoechogenicity with vascularity on US

Diffuse large B-cell lymphoma

Diffuse large B-cell lymphoma (DLBCL) is the most prevalent form of non-Hodgkin's lymphoma (NHL), and has a high incidence among the elderly, with a predilection for involving the muscles surrounding the pelvic girdle. Primary involvement of skeletal muscle by DLBCL is exceptionally rare, and accounts for 0.5% of all extranodal lymphomas.^[8] US of the same may reveal diffusely bulky muscle, and may sometimes show a heterogeneous, hypoechoic variably defined mass in the substance of the muscle. On CT [Figure 15A and B], the affected muscle(s) appears bulky and shows diffuse contrast enhancement. MRI [Figure 16] is considered superior in imaging of primary muscular lymphomas. Isointensity to muscle on T1W images and hyperintensity on T2W images are seen.

Atypical lipomatous tumors

Atypical lipomatous tumors (ALT) is the new term that has replaced the older "liposarcoma" (according to the World

Health Organization classification of soft-tissue tumors in 2013^[9] [Figure 17A and B]. They are the second most

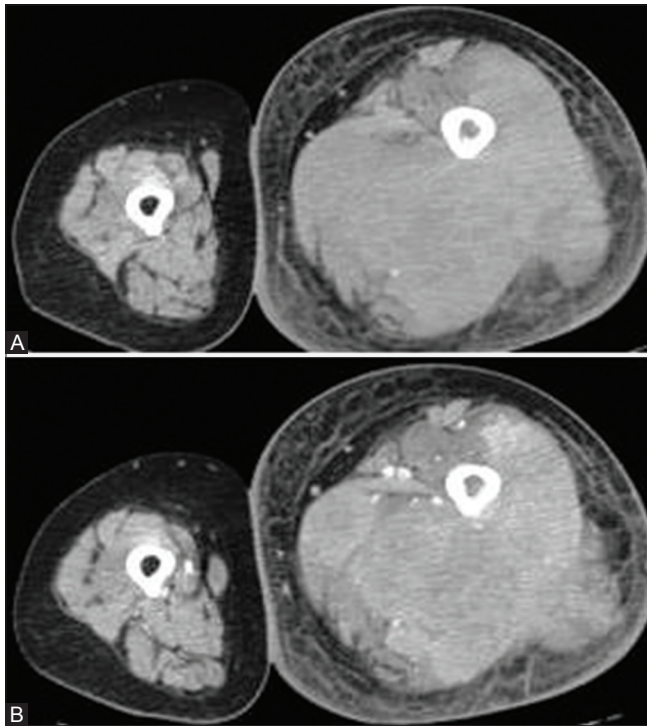


Figure 15 (A and B): Primary muscular B-cell lymphoma in a 64-year-old female with progressive swelling and weakness of the left thigh. (A) Unenhanced axial CT image reveals a large iso-attenuating lesion in the intramuscular plane of the posterior thigh; (B) CECT images show heterogeneous enhancement of the lesion

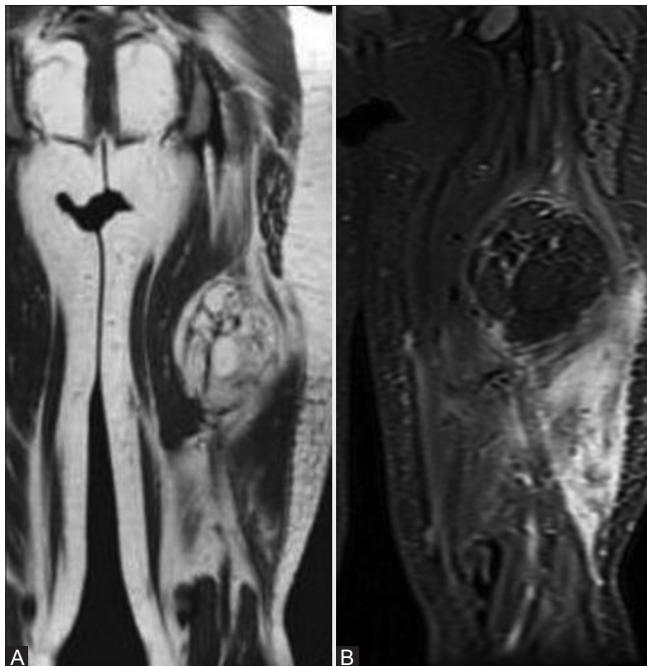


Figure 17 (A and B): ALT in a 52-year-old female with progressive left thigh swelling and neuropathic pain. (A) Coronal T1W image shows a lobulated, well-defined fat-intensity lesion within the left vastus intermedius; (B) Coronal STIR image shows fat signal attenuation within the lesion with muscular edema

common soft-tissue sarcoma, accounting for 10–35% of all cases. Lesions are commonly intramuscular, and involve the lower extremity (i.e., thigh) more frequently than the upper. On US, a heterogeneous, multilobulated, typically well-defined mass is noted. CT and MR show a well-defined, lobulated, predominantly fat-intensity lesion with foci of nonadiposity within. Nonlipomatous components are most often seen as prominent thick septa (>2 mm) that may show nodularity, and this serves to differentiate it from a lipoma. Moderate to marked enhancement of the septa is noted with contrast.

Secondary intramuscular malignant tumors

Metastases to skeletal muscle are rare, and are seen in 16–17.5% of all autopsies of cancer patients with widespread metastatic disease, predominantly in the musculature of



Figure 16: Primary muscular non-Hodgkin's lymphoma in a 67-year-old female with nonspecific abdominal pain. Coronal STIR image shows diffusely bulky and hyperintense right iliopsoas and gluteus maximus

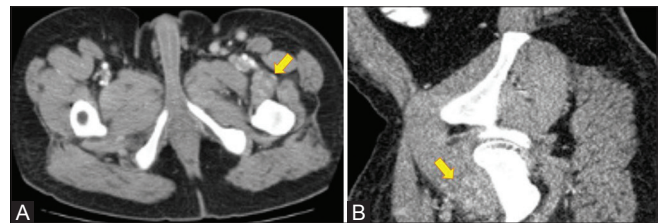


Figure 18 (A and B): Muscular metastasis in a 70-year-old male with unknown primary. (A) CE axial CT image and (B) sagittal reconstruction image show multiple ill-defined enhancing lesions within a bulky insertion of the left iliopsoas

the trunk. The common primaries involved are genital tumors (24.6%), gastrointestinal tumors (21.3%), urological tumors (16.4%), and malignant melanoma (13.1%), bronchial carcinoma (8.2%), thyroid gland carcinoma (4.9%), and breast carcinoma (3.3%).^[10,11]

On US, muscular metastases are noted to be variably defined, hypoechoic masses within the substance of the muscle. The CT appearance [Figure 18A and B] is usually that of hypoattenuating lesions with variable definition and contrast enhancement.

On MRI [Figure 19A and B], skeletal metastases appear isointense to muscle on T1 images, show heterogeneous signal with perilesional edema on T2 images, and show peripheral enhancement on contrast images [Figure 20A–C]. A rare tumor to metastasize muscle is synovial sarcoma. Despite its name, synovial sarcoma is not of synovial origin, and is usually extraarticular. Common occurrence is within the soft tissue around the joints of the extremities (lower limb commonly) [Figure 21A–D]. The ultimate diagnosis of a suspected muscular metastasis, however, is via histopathology.

Myositis ossificans

Myositis ossificans (MO) is the occurrence of heterotopic ossification that usually follows trauma to the associated

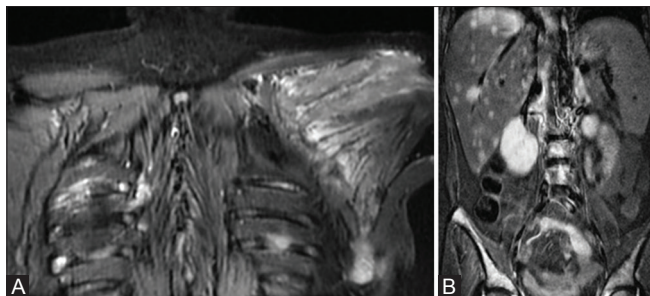


Figure 19 (A and B): Muscular metastasis in a 44-year old female with breast carcinoma. (A) Coronal STIR image shows diffusely bulky, hyperintense muscles of the left infraspinatus and supraspinatus, representing muscular metastasis; (B) Coronal STIR image of abdomen reveals hyperintensities within the liver representing metastases

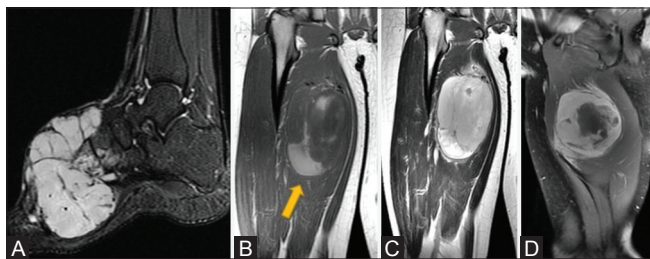


Figure 21 (A-D): Synovial sarcoma of foot with metastasis in a 57-year-old male. (A) Sagittal STIR: hyperintense lesion involving forefoot; (B) Coronal T1W image thigh: iso-hyperintense metastasis (arrow) involving adductor magnus; (C) Coronal T2W image reveals hyperintensity; (D) Sagittal CE T1W FatSat image: enhancement with central necrosis

joint. It may also occur without history of trauma, in paraplegics. MO *circumscripta* is heterotopic calcification that follows trauma, whereas MO *progressiva* (now known as fibrodysplasia ossificans *progressiva*) is a rare inherited disorder inherited predominantly via sporadic mutation.

Myositis ossificans circumscripta

MO *circumscripta* on radiographs appear as peripherally ossified, centrally lucent masses usually found around joints. Calcification usually starts by approximately 2 weeks, and assumes its classical appearance by 2 months. CT findings [Figure 22A] are similar, demonstrating calcification that proceeds from the periphery to the center.

On MRI [Figure 22B–D], features vary with the age of the lesion. Early MO is T1 isointense to muscle, T2 hyperintense peripherally, and heterogeneously hyperintense centrally. Late MO resembles bone and shows low peripheral and high central intensity on both sequences. While early MO may heterogeneously enhance, late MO usually does not.



Figure 20 (A-C): Muscular metastasis in a 21-year-old male with Ewing's sarcoma. (A) Coronal T1W image shows a hypointense lesion in left latissimus dorsi (arrow); (B) Coronal T2W image shows mild hyperintensity; (C) CE T1W image shows peripheral enhancement. Also noted is involvement of left iliac bone

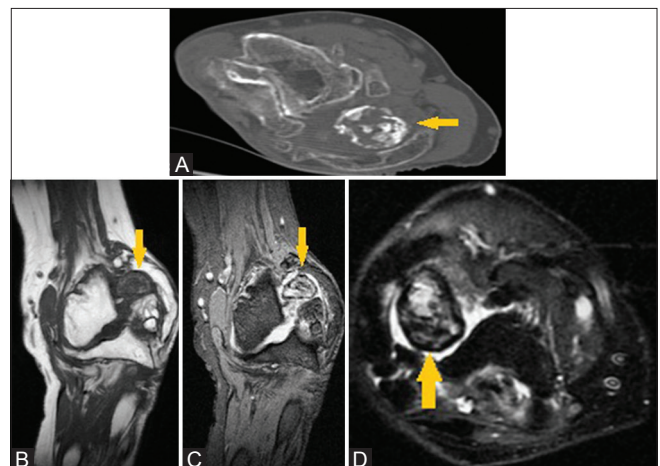


Figure 22 (A-D): Myositis ossificans *circumscripta* in a 33-year-old female with history of elbow trauma. (A) Axial CT shows peripheral calcification (arrow); (B) Coronal T1W, and (C) Coronal gradient echo images show periarticular mineralization; (D) Axial STIR shows heterogeneous hyperintensity

Myositis ossificans progressiva

MO progressiva [Figure 23] is characterized by insidious fibrosis and calcification of muscles, ligaments, and tendons that ultimately proves fatal due to involvement of the respiratory musculature.

Intramuscular hematomata

Intramuscular hematomata may be spontaneous, or secondary to hemorrhagic diathesis, anticoagulant therapy, trauma, tumor, recent surgery, or biopsy. In muscular trauma, blunt injury is commonly implicated. US imaging of acute mild muscular trauma may reveal focal isoechoic muscle swelling against the background of the undamaged muscle tissue. The appearance of more severe contusions with hematoma formation varies with the elapsed time: within 24 hours, hematomata may appear both hypo- and hyperechoic. In the following days, hematomata may appear hypo- or anechoic, until coagulation renders them inhomogeneous. Ultimately, they resolve, sometimes with residual scarring. In case of incisive injuries, US may reveal disrupted muscle fibers with local hematoma [Figure 24A].

CT images [Figure 24B and C] show increased bulk of the affected muscle, with intramuscular hyperdensity (>40 HU), representing acute bleed. As it develops, a focal hypodensity takes its place. MR appearance [Figure 25A and B] varies with the age of the hematoma: acute hematomata show iso-hypointensity to muscle on T1W; and slightly hypo- or hyperintensity on T2W. Subacute hematomata show three levels of intensity on T1 images: a low-intensity capsular sign, high-intensity in the peripheral zone, and central isosignal.

As the hematoma develops, the central and peripheral signal intensities tend to decrease, on both T1W and T2W sequences. Chronic hematomata may present with



Figure 23: Myositis ossificans progressiva (fibrodysplasia ossificans progressiva) in a 26-year-old male with progressive breathing difficulty. Unenhanced axial CT of the chest reveals extensive muscular ossification involving the left anterior chest and upper limbs. Band-like ossification is noted involving the interscapular region

hypointense collections on T1W images and hyperintense on T2W images.^[12] In all cases of suspected hematoma, clinical/sonological follow-up must be done till resolution, in order to conclusively rule out a hemorrhagic sarcoma.

Intramuscular vascular malformations

Vascular malformations need to be differentiated from true vascular neoplasms such as hemangiomas, as this holds therapeutic and prognostic significance. Vascular malformations are classified on the basis of MRI as being either high-flow malformations [arteriovenous (AV) malformations, AV fistulae], or slow-flow malformations (venous, lymphatic, capillary, or combined).

On US, venous malformations appear as multiple compressible dilated tortuous veins clumped together. Color Doppler flow [Figure 26A] and venous waveform should be sought within this lesion, which, if present, is diagnostic. Changes in flow are noted with maneuvers such as gravity dependency and Valsalva. However, due to sluggish flow, flow may be absent altogether. Phleboliths may be seen [Figure 27], which is often the distinguishing characteristic between an arteriovenous malformation and a hemangioma, the latter of which tends to contain intralesional fat. On MRI, the slow-flow channels are seen as T2-hyperintense lobules or serpiginous channels. Contrast MR shows delayed, heterogeneous enhancement [Figures 26B and C, 28A–C].

Myocysticercosis

Cysticercosis is a parasitic infection caused by ingestion of the eggs of *Taenia solium* or *Taenia saginata*, transmitted through the feco-oral route. Humans are a definitive host

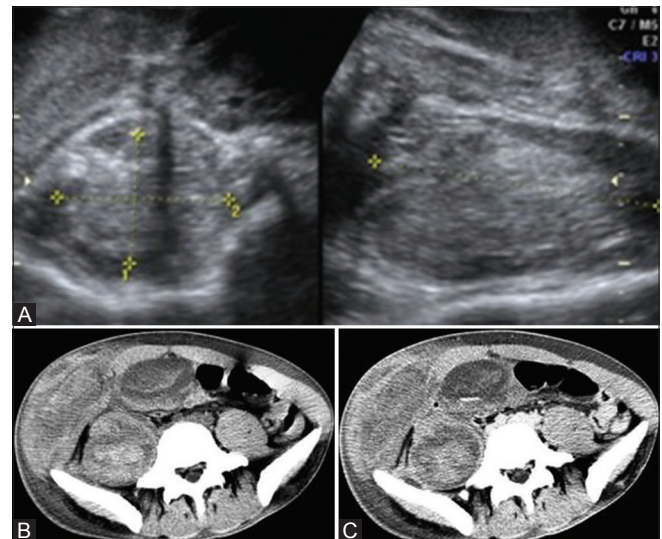


Figure 24 (A-C): Hematoma in a young male with history of trauma to the abdominal wall. (A) Heteroechoic psoas hematoma on ultrasound; (B) Unenhanced axial CT image shows heterodense collections within the right psoas muscle, and anterolateral abdominal musculature; (C) Axial CECT of the pelvis shows lack of enhancement

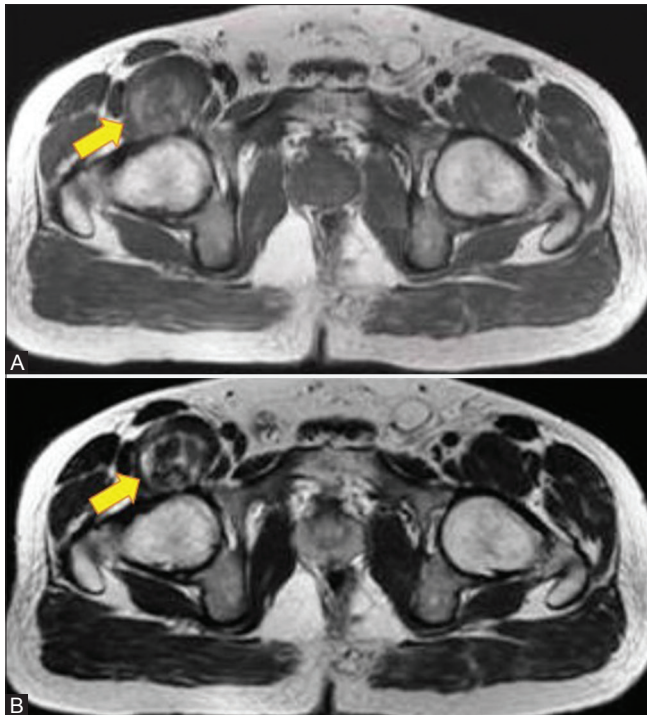


Figure 25 (A and B): Subacute hematoma in an 18-year-old male with hemophilia. (A) Axial T1W image and (B) Axial T2W image of the pelvis shows a heterointense collection (arrow) near the insertion of the right iliacus

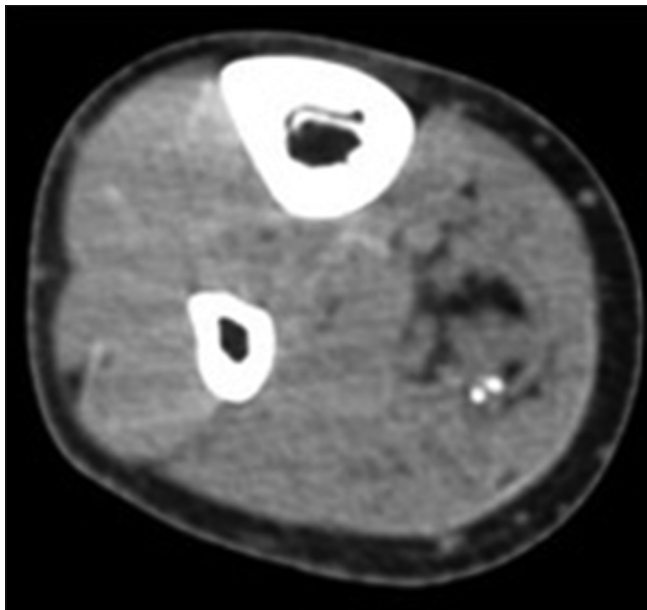


Figure 27: Slow-flow venous malformation in the belly of right gastrocnemius in a 38-year-old male with occasional dragging calf pain. Axial unenhanced CT of the leg shows an iso-to-hypodense lesion with phleboliths, characteristic of arteriovenous malformation. Hemangiomas, in contrast, tend to contain intralesional fat

for the adult parasite. Cysticerci are the larval stage of the tapeworm, and may be found disseminated in neural and soft tissue, where it incites an inflammatory reaction and may calcify over extended periods of time. The clinical differential diagnosis for soft-tissue cysticercoses may be

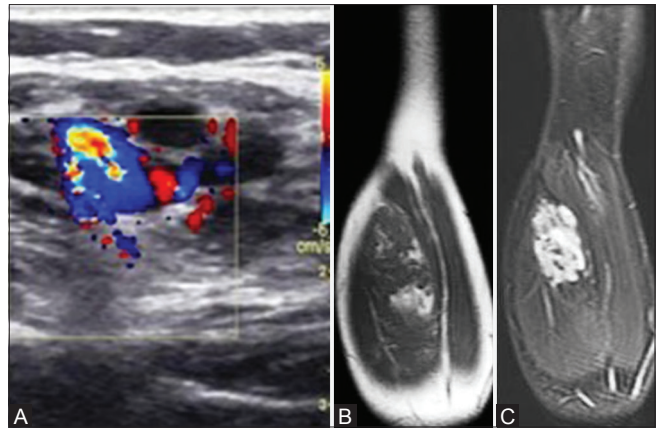


Figure 26 (A-C): Slow-flow vascular malformation in lateral head of gastrocnemius in a 34-year-old male with chronic, progressive, painless calf swelling. (A) Marked lesion vascularity on Doppler; (B) Coronal T1W image reveals an isointense lesion; (C) Coronal STIR image shows hyperintensity

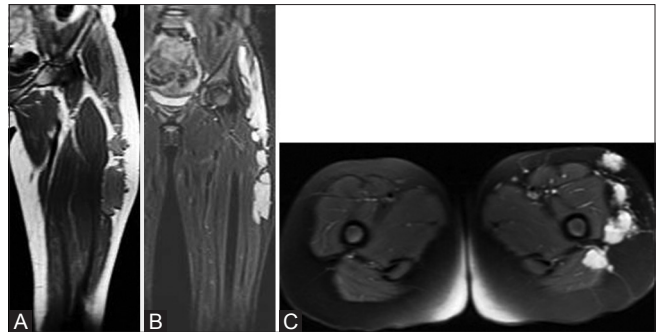


Figure 28 (A-C): Slow-flow venolymphatic malformation of the left vastus lateralis and glutei in a 30-year-old female with soft, compressible lateral thigh swelling. (A) Coronal T1W image of the left lower limb shows a large isointense lesion; (B) Coronal STIR and (C) axial T2W images show hyperintensity

lipoma, epidermoid cyst, abscess/pyomyositis, tuberculous lymphadenitis, myxoma, neurofibroma, or fat necrosis.

Diagnosis may be made on the basis of radiographs, which may show multiple calcified specks (so-called “rice-grain” calcification) in the substance of muscle. US may reveal a well-defined lesion with surrounding perilesional edema, often revealing the parasite’s scolex within [Figure 29].

On MR [Figure 30A and B], it appears hypointense on T1W and hyperintense on T2W images. Peripheral rim enhancement of the cyst wall may be seen. Intramuscular cysts are oriented in the direction of the muscle fibers. The scolex may be seen as a tiny hypointense speck within the hyperintense cyst.^[13] Presence of such a lesion in a patient with known neurocysticercosis should always raise suspicion for myocysticercosis.

Intramuscular endometriosis

Endometriosis is the presence of endometrial tissue outside the uterine cavity. Abdominal wall endometriosis may occur following the implantation of endometrial cells into the soft

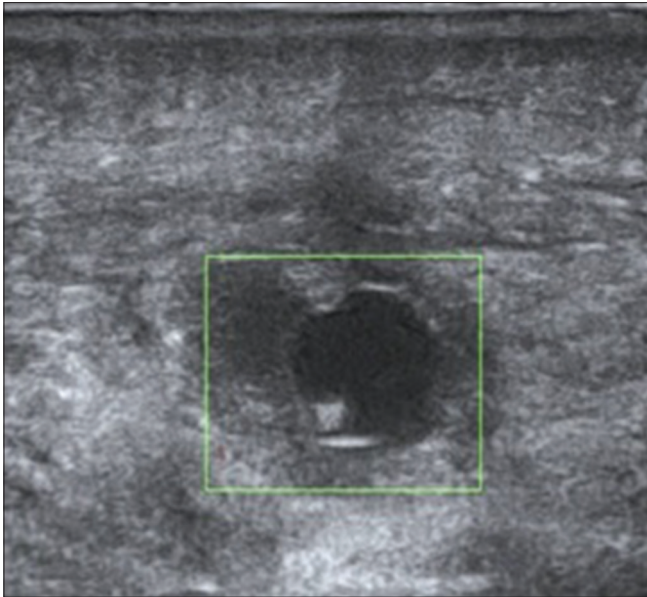


Figure 29: Myocysticercosis in a 30-year-old male with chronic calf swelling and tenderness. Ultrasound image shows a well-defined ovoid intramuscular lesion with perilesional edema and a scolex within

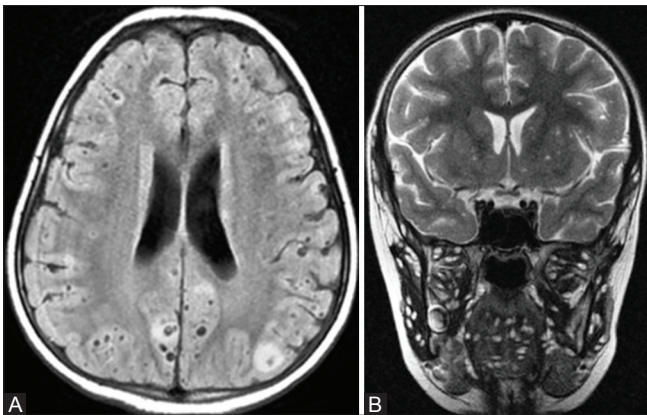


Figure 30 (A and B): Myocysticercosis in a 20-year-old female with neurocysticercosis and recurrent episodes of seizure. (A) Axial T2 FLAIR image of the brain reveals multiple parenchymal hypointensities with eccentric hyperintense scolices; (B) Coronal T2 image shows similar lesions in the extraocular muscles, muscles of mastication and tongue

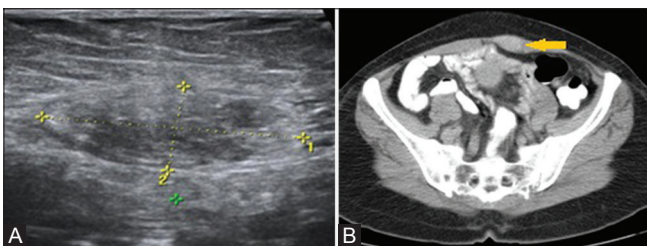


Figure 31 (A and B): Intramuscular endometriosis in a 30-year-old female with past history of cesarean section. (A) Ultrasound reveals an isoechoic intramuscular island; (B) Axial CECT of the pelvis shows the lesion within an irregularly enlarged left rectus abdominis, with heterogeneous enhancement

tissues of the abdominal wall after open uterine surgeries like cesarean sections. The incidence rate is reported at 0.4–0.1%.^[14]

US [Figure 31A] reveals a heterogeneous hypoechoic, irregularly margined lesion within the affected muscle (commonly the abdominal recti). Color Doppler may reveal flow. On CT [Figure 31B], irregularity and bulkiness of the affected muscle may be seen, with occasional hyperdense/hypodense foci within, representing the endometrial islands. MR reveals a poorly contrast-enhancing heterogeneous hypo-hyperintense area within the affected muscle, with muscle bulkiness.

Conclusion

Imaging of patients with musculoskeletal complaints may reveal the presence of various intramuscular lesions that may not be readily apparent on clinical examination. Oftentimes, a dire diagnosis may masquerade under a clinically benign presentation, and keeping in mind the various imaging characteristics of the implicated lesions would assist in coming to a timely, reasonably accurate conclusion about the etiology of the patient’s complaints and the severity of disease, in addition to helping sample the lesion for histopathology and in directing patient therapy.

Declaration of patient consent

The authors certify that they have obtained all appropriate patient consent forms. In the form the patient(s) has/have given his/her/their consent for his/her/their images and other clinical information to be reported in the journal. The patients understand that their names and initials will not be published and due efforts will be made to conceal their identity, but anonymity cannot be guaranteed.

Financial support and sponsorship

Nil.

Conflicts of interest

There are no conflicts of interest.

References

1. Fletcher CD, Martin-Bates E. Intramuscular and intermuscular lipoma: Neglected diagnoses. *Histopathology* 1988;12:275-87.
2. Paunipagar BK, Griffith JF, Rasalkar DD, Chow LT, Kumta SM, Ahuja A. Ultrasound features of deep-seated lipomas. *Insights Imaging* 2010;1:149-53.
3. Cohen AJ, Youkey JR, Clagett GP, Huggins M, Nadalo L, d’Avis JC. Intramuscular hemangioma. *JAMA* 1983;249:2680-2.
4. Murphey, Mark D, Sean W Smith. Imaging of musculoskeletal neurogenic tumors: Radiologic-pathologic correlation. *Radiographics* 1999;19:1253-80.
5. Escobar C, Munker R, Thomas JO, Li BD, Burton GV. Update on desmoid tumors. *Ann Oncol* 2011;23:562-9.
6. Ozbek N, Danaci M, Okumus B, Gursel B, Cakir S, Dabak N, et al. Recurrent intramuscular myxoma: Review of the literature, diagnosis and treatment options. *Turk J Cancer* 2006; 36:75.
7. Wu JS, Hochman MG. Soft-tissue tumors and tumorlike lesions:

- A systematic imaging approach. *Radiology* 2009;253:297-316.
8. Glass AG, Karnell LH, Menck HR. The national cancer data base report on non-Hodgkin's lymphoma. *Cancer* 1997;80:2311-20.
 9. Fletcher CD, Unni KK, Mertens F, editors. Pathology and genetics of tumours of soft tissue and bone. Iarc; 2002.
 10. Hwang S. Imaging of lymphoma of the musculoskeletal system. *Radiol Clin North Am* 2008;46:379-96.
 11. Acinas GO, Fernandez FA, Satue EG, Buelta L, Val-Bernal JF. Metastasis of malignant neoplasms to skeletal muscle. *Rev Esp Oncol* 1984;31:57-67.
 12. Muttarak M, Peh WC. CT of unusual iliopsoas compartment lesions. *Radiographics* 2000;20(suppl-1):S53-66.
 13. Tripathy SK, Sen RK, Sudes P, Dhatt S. Solitary cysticercosis of deltoid muscle in a child: The diagnostic dilemma and case report. *J Orthop* 2009;6:e11.
 14. Bozkurt M, Çil AS, Bozkurt DK. Intramuscular abdominal wall endometriosis treated by ultrasound-guided ethanol injection. *Clin Med Res* 2014;12:160-5.